THE IMPACT OF COOLING STRATEGIES AND FIXTURE OPTIONS ON THE THERMAL LOAD DURING LASER PROCESSING OF CARBON FIBRE REINFORCED THERMOPLASTICS

R. Staehr[1], J. Lindner[2], S. Bluemel[1], O. Meier[2], P. Jaeschke[1], O. Suttmann[1], L. Overmeyer[1]

[1]Laser Zentrum Hannover e.V., Hollerithallee 8, 30419 Hannover, Germany
Email: r.staehr@lzh.de, s.bluemel@lzh.de, p.jaeschke@lzh.de, o.suttmann@lzh.de, l.overmeyer@lzh.de
Web Page: http://www.lzh.de
[2]LASER on demand GmbH, Industriestr. 1, 30855 Langenhagen, Germany
Email: jl@laser-on-demand.de, om@laser-on-demand.de
Web Page: http://www.laser-on-demand.de

Keywords: laser cutting, thermoplastic CFRP, thermography, cooling, fixture

Abstract
This paper focusses on different fixture and cooling options and investigates their impact on the thermal load during laser processing of CFRP using a continuously emitting high-power solid state laser. Various combinations between fixtures, cooling options and process parameters were used. These options included cooling by pressurized air flow or water spraying when using uncooled fixtures with spacing under the CFRP plate. Another option included air flow or water spraying using water cooled fixtures with direct planar contact to the CFRP surface.
The surface temperatures were monitored by thermography during the cutting process, serving as an indicator for the effectiveness of the cooling options. The HAZ of selected cross-section specimens was measured, supporting the evaluation process of the cooling effectiveness.
The results revealed a distinct reduction in the surface temperatures when applying gas flow cooling compared to the absence of any cooling, while the effect of an additional water spray becomes apparent especially for an enhanced water flow. The highest heat dissipation was achieved by using a water cooled fixture. This effective cooling option enables the reduction of typically necessary delay times thus leading to higher process efficiency at a constantly low thermal load.

1. Introduction

Carbon fiber reinforced plastics (CFRPs) are widely recognized as being a great lightweight construction material e.g. for the improvement of dynamic performance in the aerospace, automotive and transportation sectors. Despite offering outstanding properties, major resistances to the use of CFRP are the high manufacturing and processing costs. Conventional machining techniques, such as milling, drilling or waterjet cutting, which are well developed for a wide variety of other materials, suffer from high tool wear, insufficient quality or their complex setup and limited flexibility when it comes to the requirements of CFRP machining [1-3]. Laser processing offers specific benefits such as highly flexible, wear free cutting thus contributing to the reduction of processing costs [4]. However, in laser processes the heat generated can lead to heat affected zones (HAZ), which might affect the mechanical properties and aging resistance. Current laser processing methods include various passes of the laser beam at high speed across the same cutting contour combined with delay times acting as cool down periods for heat dissipation [4-6]. These adapted strategies help to minimize the HAZ but also lead to low effective cutting velocities. For an improved establishment of laser based processing

Excerpt from ISBN 978-3-00-053387-7

within industry, effective cutting velocities require improvement and material-specific temperature limits must be observed with efficient and industrially applicable techniques [7]. Especially in the aviation industry limiting temperature values reached in the machining process are chosen rather conservatively. To meet these requirements and to achieve a sufficient processing efficiency, active cooling equipment might be a promising option.

2. Experimental setup

Tencate Cetex® carbon fiber reinforced organic sheets with 1.24mm thickness were used for these experiments. The thermoplastics Polyphenylene sulfide (PPS) constituted the matrix material. The material characteristics are provided in Table 1. The melting temperature of this material is at T_m=280°C while the glass transition temperature is at T_G=90°C only [8]. In most cases, the machining temperature limit for CF/PPS, recommended by customers from the aviation industry, is the glass transition T_G.

Table 1. CFRP materials used for the experimental work

Material	Fabric	Thickness (mm)	Number of layers	Fibre orientation
CF/PPS	5-harness satin weave	1.24	4	$[(0)_2,(90)_2]_T$

Laser used in the studies was a continuously emitting Trumpf TruDisk 1000, providing an output power of P_L=1kW at a wavelength of λ= 1030nm. The laser radiation was fiber guided to a collimator attached to the scan head. The beam movement was achieved by a galvanometer scanner (Trumpf PFO) which deflects the laser beam within a 2D field using mirrors. The laser beam was focused on the material surface by focusing optics with a focal length of f=135mm. Based on the optics and laser specifications the spot diameter was d_f~150µm. The experimental setup is shown in Figure 1.
Different cutting strategies exist for laser cutting of CFRP. For good cutting quality, the most common strategy is multipass cutting. The multipass strategy utilizes high speed scanning (v_s) and needs various passes on the same contour. Compared to cutting strategies with a full cut achieved by a single pass, the input energy during one pass is reduced and additional cooling periods can be added between passes. Hence, the thermal material modification can be reduced and the cutting quality increases. The parameters used for the experiments are summarized in Table 2.
The material modification, which is typically referred to as a heat affected zone (HAZ) was studied using microscopy of cross-section specimens. The measurement of the HAZ was based on the procedure given in [6]. In this publication different types of material modifications are assumed. In the present study, regardless of type of modification, only the maximum extent of the HAZ was measured. Using digital image processing, the area of the visible material modification was measured and divided by the CFRP material thickness. By this procedure an average value of the width of the HAZ was found. The measurement was done for two specimens, a mean value was calculated and additionally the minimum and maximum values are shown as error bars in Figure 10.

Excerpt from ISBN 978-3-00-053387-7

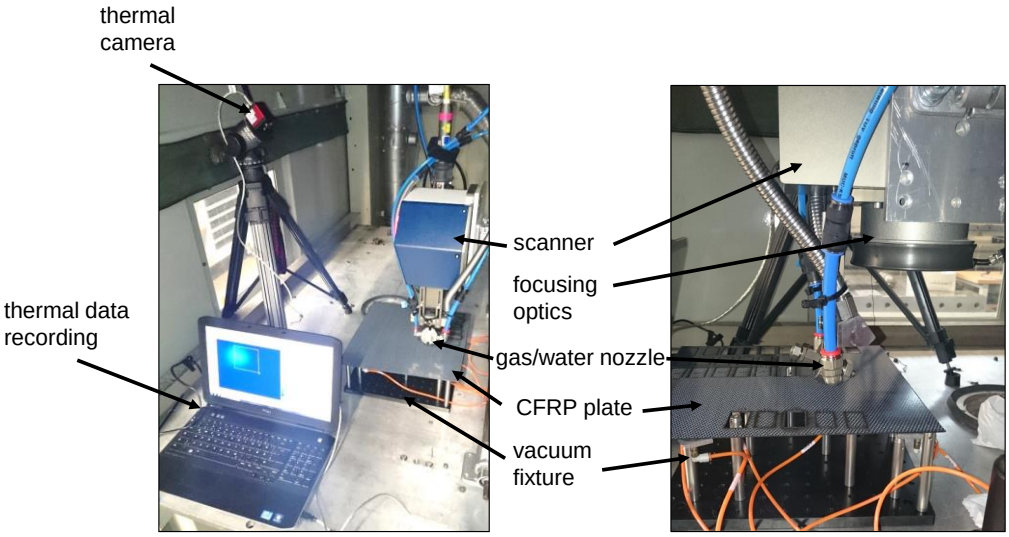

Figure 1. Experimental setup

Table 2. Experimental parameters

Parameter	
Scanning speed v_s(m/s)	0.8
Break duration t_B (s)	2 ; 5
repetitions n (-)	22
Size of the cutting contour (mm²)	20x40

For enhanced heat dissipation, various configurations of different fixtures and cooling options were used. The first option included cooling by pressurized air flow at a pressure of p~2bar across the CFRP surface. In a second option, this step was enhanced by adding a water spray in the gas flow. For the water spray two intensities were chosen. For the lower intensity the water flow was adjusted, so that no water droplets appeared on the material surface. A strong water spray was set by adjusting the flow through the nozzle to the maximum (~0.30 l/min). With this setting a droplet deposition on the surface was observed. These options were applied in a process in which a CFRP plate was held in position by a vacuum fixture. This fixture maintains a defined space between the CFRP backside and a ground plate while minimizing contact areas between CFRP and fixture (see Figure 2 a) and b)). The option was chosen to provide a maximum available area for heat dissipation by free convection. The last solution included a water cooled vacuum fixture which provided heat dissipation by direct planar contact between the entire CFRP surface and the steadily cooled fixture (see Figure 2 c) and d)). The cooling unit used for the water flow though the fixture provided water at a temperature of T=16°C and a water flow of 0.48m³/h. Both, air flow and water spray cooling were used for the cooled fixture.
For reference purposes, a measurement without any cooling and with additional delay times was made. To reveal a dependency on delay times between passes, delay times of t_p=2s and t_p=5s were used for the experiments. In absence of any cooling and without a delay time between passes, the specimen's material heats up heavily and starts burning. For the evaluation of the results the parameter set without delay time and without cooling were not included. A summarized test plan for the fixtures, cooling options and delay times is given in Table 3.

Excerpt from ISBN 978-3-00-053387-7

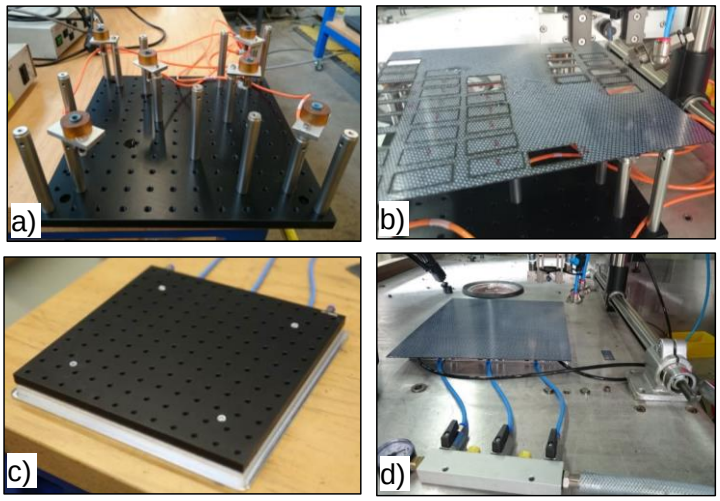

Figure 2. Fixture types used for the experiments: **a) and b)** vacuum fixture with spacing between ground plate and CFRP; **c) and d)** vacuum fixture with water cooled ground plate and direct contact to the CFRP

Table 3. Fixture and cooling options

Setup no.	Fixture type	Cooling options			
		Cooled fixture	Air	Water spray	Delay time (s)
1	with spacing	No	No	No	2
2	with spacing	No	Yes	No	2
3	with spacing	No	No	Yes	2
4	with spacing	No	Yes	No	5
5	with spacing	No	No	Yes	5
6	with spacing	No	No	Yes, Strong	5
7	without spacing	Yes, water	Yes	No	2
8	without spacing	Yes, water	No	Yes, Strong	2

The surface temperature was detected by a PIR uc 180 thermography camera from Infratec GmbH (see detailed technical specifications in Table 4). The camera was placed at a distance of s=700 mm and in an angle of incidence of α=37° when performing experiments with the fixture with spacing and at a distance of s=1240 mm and in an angle of incidence of α=32.5° when performing experiments with the fixture without spacing. An emission factor of ε=1 was chosen for all experiments. With this emission factor only a relative temperature is recorded. However, if all setups are recorded with the same setting, the measurement still points out the differences in the temperature levels.

Table 4. Specifications of the Infratec PIR us 180 thermal camera

Infratec PIR uc 180	
Detector type	Micro-bolometer
Detector resolution (Pixel)	160x120
Spectral range (µm)	7.5…13
Measuring range (°C)	-20…850
Thermal resolution (K) at 30°C	0.08
Measurement accuracy	±2% of mean value; min. 2 °C
Picture frequency at full frame (Hz)	100

Excerpt from ISBN 978-3-00-053387-7

The thermal measurement point chosen for the temperature analysis is the centre point of the specimen. An example picture showing the cutting contour and the measurement point in a thermal picture is given in Figure 3.

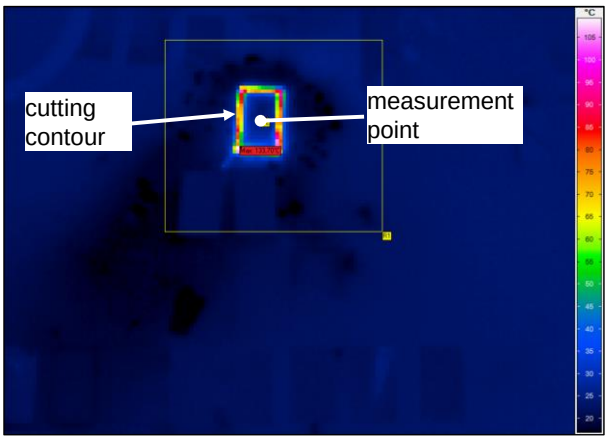

Figure 3. Cutting contour and thermal measurement point in thermography picture

3. Results and discussion

In the following paragraph the time-dependent temperature measurements on the center point of the specimen are shown and compared for the configurations given in Table 3. An exemplary overall temperature graph and its details are shown and explained in Figure 4. The local temperature peaks (Figure 4, II) within generally the upward-sloping temperature course (Figure 4, I) occur during the laser-on time, while material is removed. Each local peak stands for a single laser pass on the specimens contour. Variations in the height of the temperature peak from pass to pass can be assigned to cutting process emissions during the laser-on time which are blown into the measurement point of the thermography camera. Small peaks or saddle points within the local peaks (Figure 4, II) appear due to the laser passing the measurement point on two sides while cutting the rectangular-shaped specimen. Each laser pass peak is followed by the delay time leading to a heat dissipation in the material (Figure 4, III) before the next pass starts. Due to the variation in the height of the local peaks, for the evaluations the local minimum before the last pass is related to the cooling effectiveness.

Excerpt from ISBN 978-3-00-053387-7

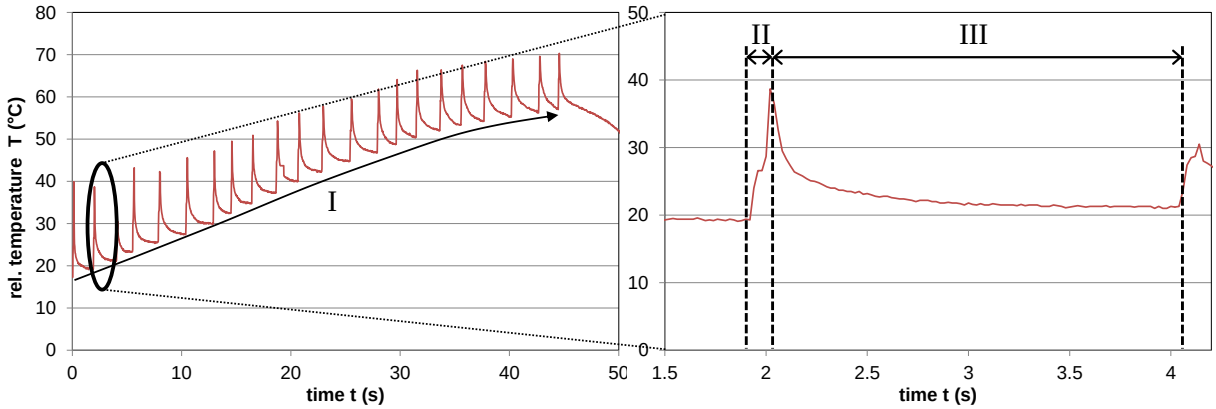

I: Increasing overall temperature level over the process duration

II: Laser-on, local peaks due to laser pass on two sides of the measurement point

III: delay time / cool down phase (here t_p=2s)

Figure 4. Time-dependent thermography temperature monitoring graph and details in the temperature course

In Figure 5 the temperature course is shown for the fixture type with spacing, a delay time of t_p=2s and different cooling configurations. The temperature level reaches a relatively high level up to T~160°C for the process setup without cooling, while lowest temperatures T<60°C were measured for air flow cooling. Although showing lower temperature levels in the first third of the process, the temperatures for water spray cooling climb up to T~90°C.

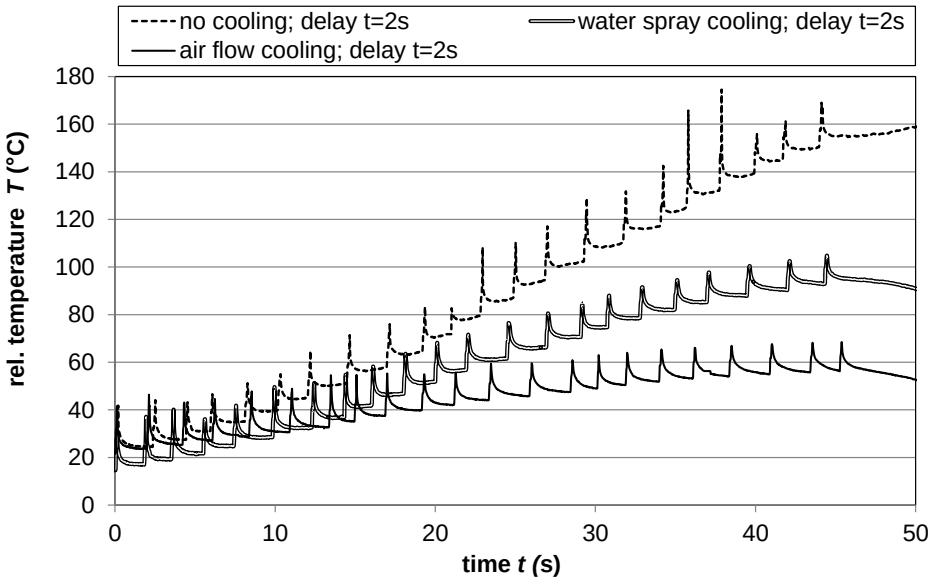

Figure 5. Time-dependent temperature course for different cooling options for the fixture with spacing and a delay time of t_p=2s

Excerpt from ISBN 978-3-00-053387-7

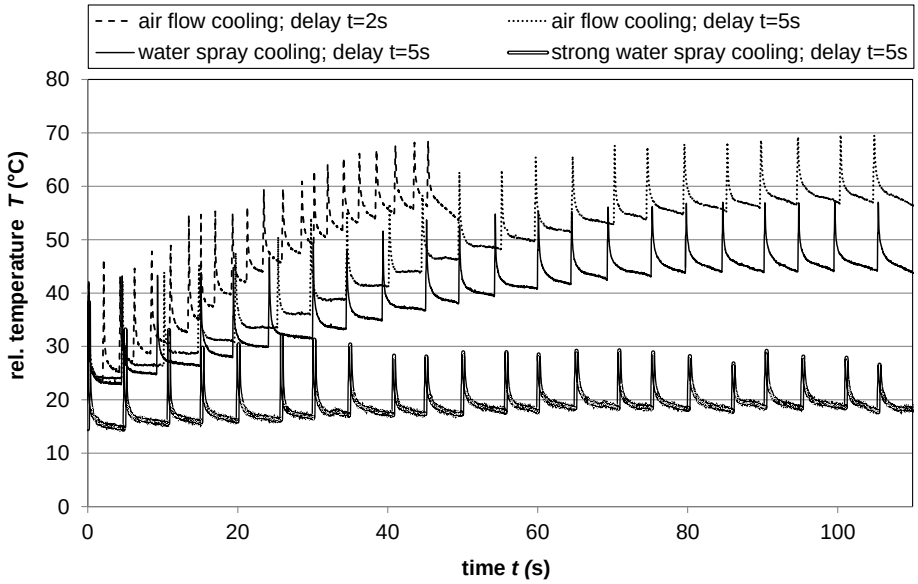

Figure 6. Time-dependent temperature course for different cooling options for the fixture with spacing and delay times of t=2s and t=5s

In Figure 6 the temperature course for a delay time of t_p=2s is compared to delay times of t_p=5s for the fixture type with spacing and different cooling configurations. Due to the increased delay time between each pass, the longer overall process time becomes apparent. Although giving more time for heat dissipation, the temperature level for the air flow cooling and a delay time of t_p=5s reaches the same level as for t_p=2s. Other than for t_p=2s, the temperature level for the water spray cooling at t_p=5s stays at levels beneath the air flow cooling. An enormous temperature reduction to levels close to room temperature is achieved by an enhanced water flow through the nozzle. However, when using this water flow adjustment, droplets remain on the CFRP surface (shown in Figure 7). These droplets might lead to a water uptake at the cutting edge and they also might lead to an additional cleaning step required after the cutting process. Nevertheless, the area effectively cooled by the water droplets becomes visible in the thermography image (see Figure 8). Due to the high amount of water on the material surface, the temperatures inside might not be deduced from the one recorded by thermography.

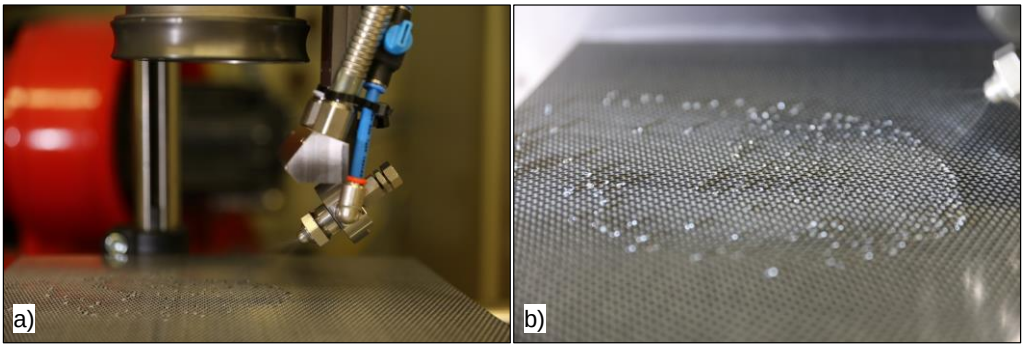

Figure 7. a) Water spray nozzle and **b)** water film and water droplets from strong water spray cooling with increased water flow

Excerpt from ISBN 978-3-00-053387-7

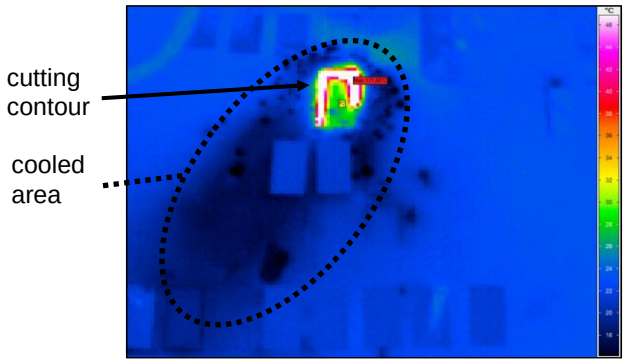

Figure 8. Visible effect of the water spray cooling in a thermal image

As shown in Figure 9, the cooling effectiveness can be further increased by the use of an actively water cooled fixture. For identical delay times the temperature level for the cooled fixture stays below the values of the air flow cooling and also below the values of the water spray cooling at higher delay times of t_p=5s. However, similar to t_p=2s, the effectiveness can be maximized by an enhanced water spray.

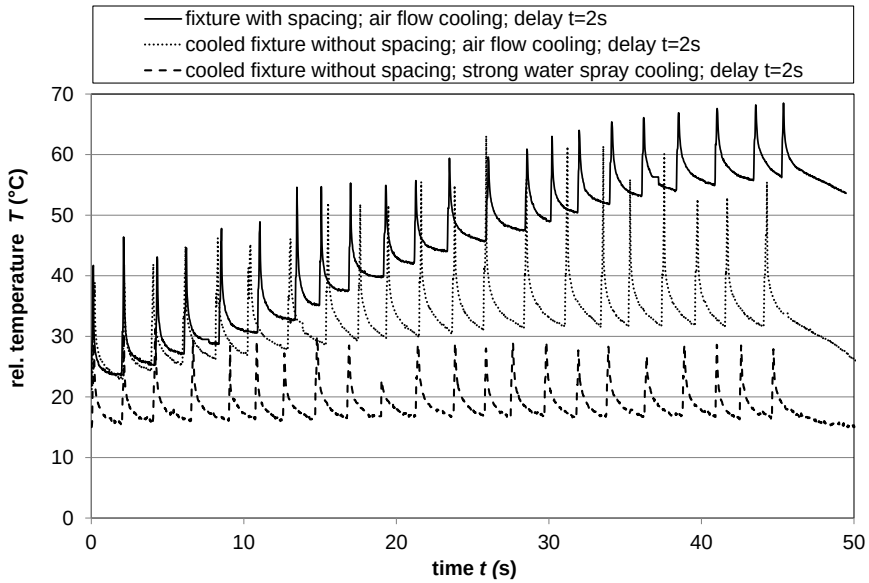

Figure 9. Time-dependent temperature course for different cooling options for the fixture with spacing and cooled fixture without spacing; delay time t_p=2s

In the last step the average HAZ for chosen specimens was measured and related to the temperature recordings (see Figure 10). Here, a slightly different behavior is observed. Although showing lower temperature levels than the water spray cooling, the air flow cooling for the fixture with spacing shows the widest HAZ, although still having overlapping error bars. In contrast to that, the air flow cooling at an increased delay time of t_p=5s, reaching temperature levels identical to the air flow cooling at a delay time of t_p=2s, has a HAZ width distinctly lower than for the short delay time and comparable to the water spray cooling at the same delay time. The differing behavior might be assigned to the local cooling effect of the air flow and water spray cooling which is mainly limited the material surface. The lowest HAZ values were measured for the strong water spray for both, the uncooled fixture with spacing and the cooled fixture without spacing. Additionally, very low HAZ values were observed for the cooled fixture and air flow cooling at t_p=2s. These values are slightly higher than for the strong water spray but still clearly below the air flow cooling on an uncooled fixture at the same delay times. It can be concluded that a cooled fixture leads to a similar HAZ extent at reduced delay times and

Excerpt from ISBN 978-3-00-053387-7

without the usage of a strong water spray. Hence, a cooled fixture might measurably contribute to lower process times and process efficiency.

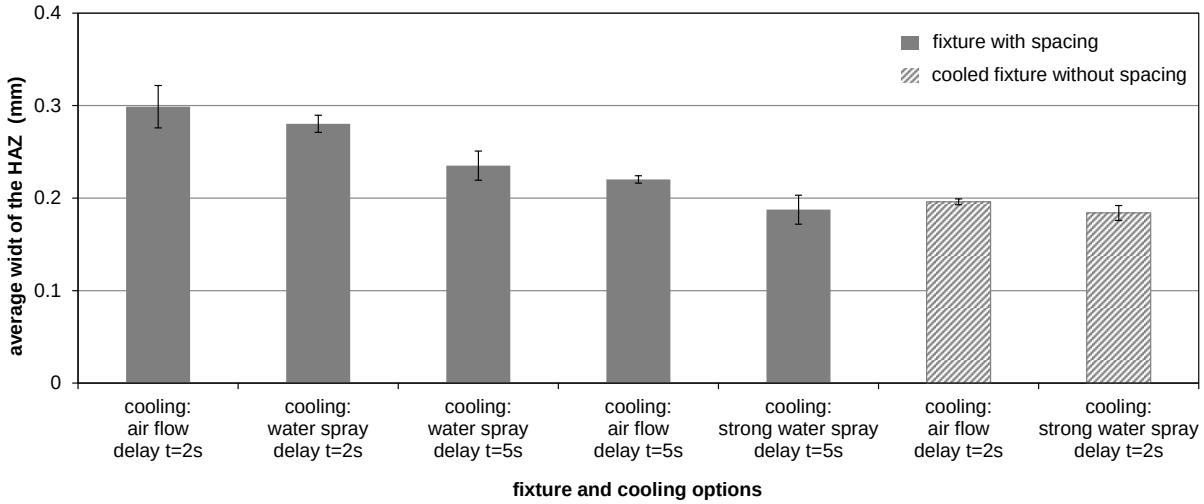

Figure 10. Average width of the HAZ for different fixture and cooling options

4. Conclusions

In this paper, investigations were carried out on the cooling effectiveness of different fixtures and cooling options while laser cutting of CFRP (CF/PPS). The configurations included cooled fixtures with direct contact to the CFRP, uncooled fixtures with spacing, air flow cooling and water spray cooling on the material surface as well as different delay times used in the multipass cutting process. The effectiveness was evaluated by means of synchronous temperature measurement on the material surface and by a following measurement of the HAZ extent. It was shown that the water spray and the air flow cooling do have a distinct effect on the material temperatures compared to no cooling. In contrast to the water spray cooling, an increased delay time did not have an effect on the temperatures when using air flow cooling. In case of the HAZ, a longer delay time did lead to a measurably reduced width. This effect was assumed to be caused by the local surface cooling of the air flow and water spray cooling. The lowest temperatures and HAZ widths were observed for long delay times and water spray cooling with an enhanced water flow. However, this method led to droplets on the material surface, which may cause a water uptake or which might lead to an additional cleaning step after the cutting process. The most effective cooling method was the cooling by the water cooled fixture combined with an air flow cooling. This method led to very low temperature levels and HAZ widths close to those of strong water spray cooling although using shorter delay times. Hence, this configuration measurably contributes to lower process times and process efficiency. However, the direct contact might lead to problems once the material is cut through and the laser beam directly interacts with the metal surface of the fixture. Later setups could add groves for the cutting contour to avoid a damage of the fixture or the CFRP part.
Since an enhanced temperature development has been experienced for materials with higher thicknesses, further investigations should focus on these materials. Lasers with higher output power, which are often used for the cutting of CFRP will also be included in future investigations.

Excerpt from ISBN 978-3-00-053387-7

Acknowledgments

The authors would like to thank the German Federal Ministry of Education and Research (BMBF) for funding these investigations within the project Co-Compact (Eurostars Ref: E!7500, FKZ:01QE1232B und FKZ:01QE1232A) and the German Aerospace Center (DLR e.V.) for their support.

References

[1] J. Y Sheikh-Ahmad. Machining of polymer composites. Springer, New York, 2009.
[2] D. Che, I. Saxena, P. Han, P. Guo, K. F. Ehmann. Machining of Carbon Fiber Reinforced Plastics/Polymers: A Literature Review. *Journal of Manufacturing Science and Engineering*, 136(3), 034001, 2014.
[3] M. Hashish. Trimming of CFRP Aircraft Components, *WJTA-IMCA*, editor. American WJTA-IMCA Conference & Expo, 2013.
[4] F. Fischer, S. Kreling, D. Blass, R. Staehr, S. Bluemel, P. Jaeschke, K. Dilger. Laser material machining of CFRP - An option for damage-free and flexible CFRP processing? *J. P. Davim (Ed.): Machinability of fiber-reinforced plastics*. De Gruyter, p. 1-29, Berlin / Boston, 2015.
[5] S. Bluemel, P. Jaeschke, O. Suttmann, O. Overmeyer Comparative Study of Achievable Quality Cutting Carbon Fibre Reinforced Thermoplastics Using Continuous Wave and Pulsed Laser Sources. *8th International Conference on Laser Assisted Net Shape Engineering LANE 2014*, 56(0), 1143–52, 2014.
[6] R. Staehr, S. Bluemel, P. Hansen,P. Jaeschke, O. Suttmann, L. Overmeyer. The influence of moisture content on the heat affected zone and the resulting in-plane shear strength of laser cut thermoplastic CFRP. *Plastics, Rubber and Composites*; 44(3), 111–6, 2015.
[7] S. Bluemel, R. Staehr, P. Jaeschke, O. Suttmann and L. Overmeyer. Correlation of internal and surface temperatures during laser cutting of epoxy-based carbon fibre reinforced plastics. *Journal of Reinforced Plastics and Composites*; 34: 662–671, 2015.
[8] Data Sheet Tencate Cetex

Excerpt from ISBN 978-3-00-053387-7